KSME International Journal, Vol. 16 No. 10, pp. 1253~1263, 2002

The Control System Modeling and Experiment for the Tele-operated Unmanned Vehicle

Duk Sun Yun*, Woon Sung Lee, Jung Ha Kim

Graduate School of Automotive Engineering, Kookmin University, 861-1, Chungnung-dong, Sungbuk-gu, Seoul 136-702, Korea

The control system design and modeling of an unmanned vehicle by means of a new concept for better performance through a tele-operation system is suggested by sensor fusion. But, the control of a real vehicle is very difficult, because the system identification of the vehicle is hard to find the unknown factors and the disturbances of the experimental environment. For the longitudinal and lateral controls, the traction system and steering system models are set up and a tuning method to find the gain of the controller by experiments is presented. In this research, mechanical and electronic parts are implemented to operate the unmanned vehicle and data reconstruction method of information about the environment data coming from several sensors is presented by data plot for the vehicle navigation. This paper focuses on the integration of tele-operated unmanned vehicle. This vehicle mainly controlled lateral and longitudinal directions with actuators for controlling vehicle movement and sensors for the closed-loop controlled system.

Key Words : Unmanned Vehicle, Driving Simulator, Tele-Operated Vehicle

Nomenclature

β_f : Side Slip Angle of Front Wheel
β_r : Side Slip Angle of Rear Wheel
δ : Steering Angle
τ : Torque of DC Motor
ω : Angular Velocity of DC Motor
f : Friction Constant of DC Motor
i_a : Magnetic Core Current of DC Motor
i_f : Magnetic Current of DC Motor
I : Yaw Moment of Vehicle
J : Inertia of DC Motor Torgue
k_f : Cornering Force of Front Wheel
k_r : Cornering Force of Rear Wheel
k_t : Coefficient of DC Motor
k_v : Inverse Electricity Generation Constant
l_f : Length from Gravity Center Point to Front Wheel
l_r : Length from Gravity Center Point to Rear Wheel
L_a : Inductance Component of Magnetic Windings
m : Total Mass of Vehicle
r : Yaw Angular Velocity
R_a : Internal Resistance
Y_{f1}, Y_{f2}: Lateral Force of each Front Wheel
Y_{r1}, Y_{r2}: Lateral Force of each Rear Wheel
u : Input Voltage
v_a : Input Voltage of DC Motor
v_k : Induced Inverse Generation of Electricity

* Corresponding Author,
E-mail : autocars@chollian.net
TEL : +82-2-916-0991; **FAX** : +82-2-916-0991
Graduate School of Automotive Engineering, Kookmin University, 861-1 Chungnung-dong, Sungbuk-gu, Seoul 136-702, Korea. (Manuscript **Received** October 4, 2001; **Revised** July 26, 2002)

1. Introduction

Today, an unmanned vehicle and the social infrastructure related researches are in fashion over the world. An autonomous vehicle can drive itself to the desired destination without aid of social infrastructures and driver operations, thus it is possible to move without help of other equipments all but sensors or actuators. But the

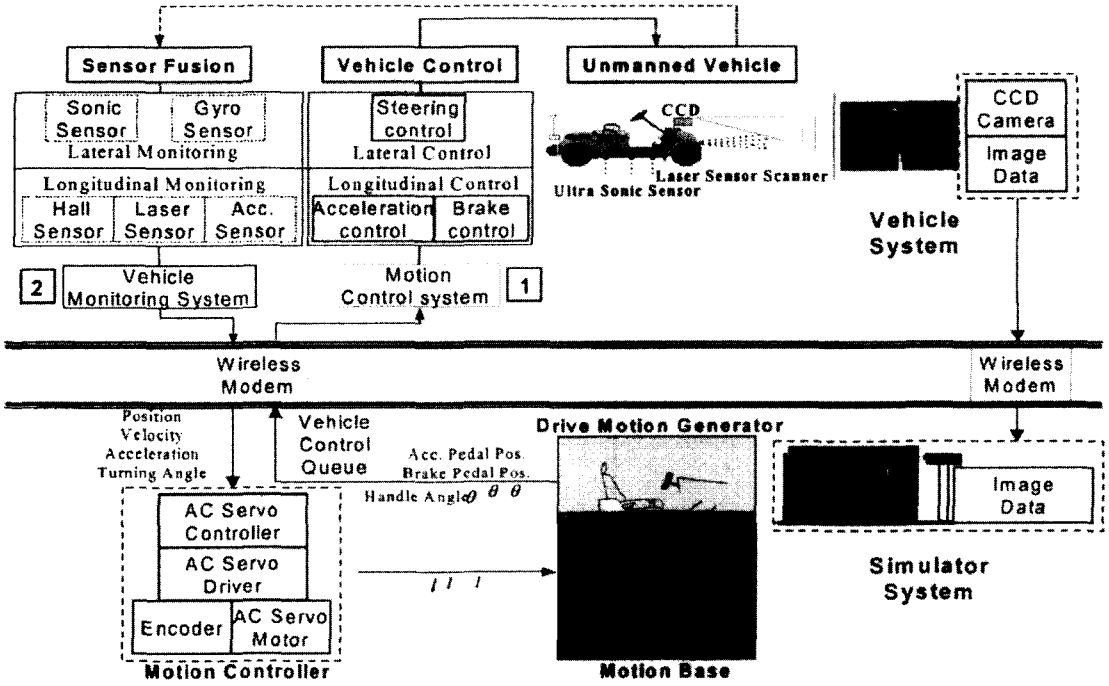

Fig. 1 Concept of tele-operated vehicle system for a driving simulator

system stability is uncertain and the expenditure is too expensive to go by itself yet and it requires expensive hardware systems, real time monitoring techniques and multiple control techniques. Thus, the electronic control related research topics of a vehicle are prevalent to all over the world, because the convenience of a driver, fatigue and stress of long time driving causing accident and efficient of road capacities. The main element of the unmanned vehicle is an actuator for operating of each hardware system and a sensitive sensor. The integration of these systems with algorithm is very important. In a hardware system, laser radar sensor or scanner detects long distance obstacles and makes out the front environment of the vehicle (Yun and Kim, 1999 ; 2000 ; 2001).

This research is focused on the system design and development of a reliable unmanned vehicle, especially, multi sensor fusion, characteristic analysis, modeling of the vehicle and controller design and parameter tuning for the performance improvement. In Fig. 1, the data flow for the interaction of the unmanned vehicle with the driving simulator and the concept of this research are presented. The data, i.e., acceleration, velocity, position, orientation, heading angle and environment information coming from range detector of the unmanned vehicle are evaluated and transmitted to the driving simulator via a wireless modem. These data are converted to each actuator's length, the velocity and acceleration of the simulator and the driving simulator simulate the unmanned vehicle's motion. In addition, the driver riding on the driving simulator feels the motion of the unmanned vehicle, watching the image data coming from the CCD camera equipped on the unmanned vehicle. The driver may control the driving motion generator, steer angle, acceleration pedal and brake pedal position of the simulator cockpit, yielding the vehicle control queue. These vehicle control queue data transmitted to the unmanned vehicle again. Finally, the vehicle controlled by a driver on the driving simulator, makes a closed loop system (Yun and Kim, 2000).

This paper is organized as follows: In Chapter 2, we represent the basic configuration and structure of the unmanned vehicle. In addition, the sub control system and sensor system are designed in the chapter. Chapter 3 deals with the experimental

results of each controller for the traction and steering system, and the achieved performance improvement is evaluated by a parameter tuning method.

2. System Configuration

2.1 Control System

Figure 2 shows the flow [1] of Fig. 1, which represents the main theme of this research. The driver's control motion for the vehicle control on the simulator, which is acceleration pedal position input and brake pedal position input, generate the voltage variation of variable resistance. It is converted to digital signals, and the steering input signal comes from the encoder because the steering input is rotational angular data, which signal requires rotational position and direction (Yun and Kim, 200 ; 2001 ; Shim, 2001).

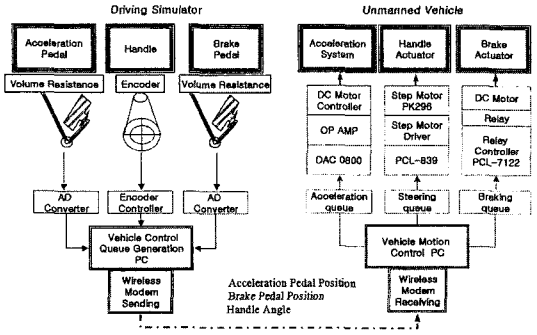

Fig. 2 Block diagram of motion control system

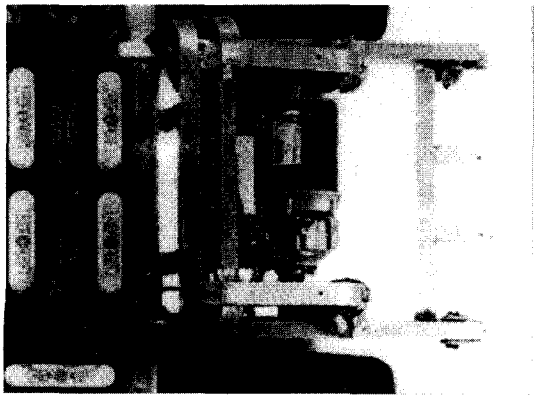

Fig. 3 DC Motor for traction system

2.1.1 Velocity control

In this research, the unmanned vehicle is an electric vehicle with a DC motor. Motor driving system controls the input voltage of the motor by digital signal processing, which comes from PC, generating current and it is converted to the corresponding voltage by a D/A converter. Figure 3 shows the traction system of the unmanned vehicle. The direct input signal control of the DC motor is easier than that of the acceleration pedal position control.

Vehicle velocity is calculated from the spinning wheel, which is produced by counting a rising signal edge at unit time, coming from hall sensor. On the basis of this data, the total driving distance can be calculated and velocity profile of the vehicle's driving locus can be generated for the path planning. Figure 4 shows the traction system model, which is an equivalent circuit model for the more precise control (Kim, 2001).

Torque of the DC motor τ is proportional to $i_a(t)$, but if is constant, because magnetic current does not vary. Thus, τ can be written by

$$\tau = k_t i_a = J\frac{d\omega}{dt} + f\omega \tag{1}$$

If it is assumed that all initial conditions are zero and R_a, k_v are constants, then the Laplace transformed equations are given as follows :

$$U(s) = k_a V_a(s) \tag{2}$$

$$V_a(s) - V_k(s) = (R_a + L_a s) I_a(s) \tag{3}$$

$$V_k(s) = k_v \Omega(s) \tag{4}$$

$$\tau = k_t I_a(s) = (Js + f)\,\Omega(s) \tag{5}$$

where, J, R_a, and L_a are hard to find out as numerical values. Therefore, it can be decided

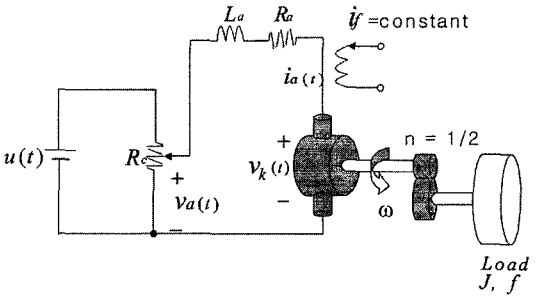

Fig. 4 Wire model of traction system

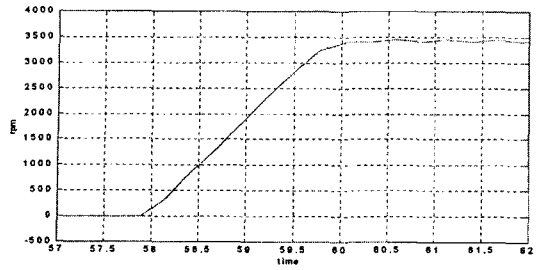

Fig. 5 Motor RPM profile

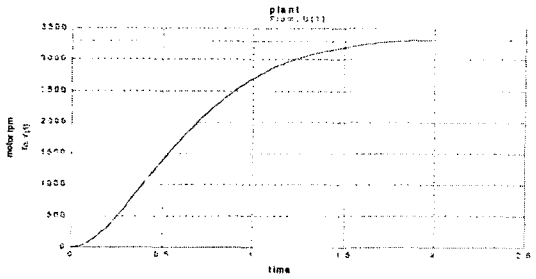

Fig. 6 Simulation result via transfer function

with the results of experiments as an approximate value, composing transfer function perfectly. Figure 5 shows the acquired velocity data after applying step input to the motor. Based on this result, the natural frequency and damping ratio are to be known for the transfer function. The transfer function of the DC Motor is given by

$$G(s)=\frac{\Omega(s)}{U(s)}=\frac{5866.575}{s^2+4.55s+7.111} \qquad (6)$$

Figure 6 shows the simulation result of MATLAB[R] based on the transfer function of Eq. (6), which means the data trend of the DC motor. It verifies that the transfer function fits well the experiment results with the similarity of both data trends.

2.1.2 Steering Control

Figure 7 shows the steering control system with a step motor using timing belt, attached on the steering column, which has a reliable angular displacement and angular velocity, even acceleration. In order to keep the lane for the lateral control, the unmanned vehicle needs standard signal as a reference for going straightly without leaning to one side. If not, it might generate a topological error of navigation. A gyroscope can

Fig. 7 2-Phase step motor system for lateral control

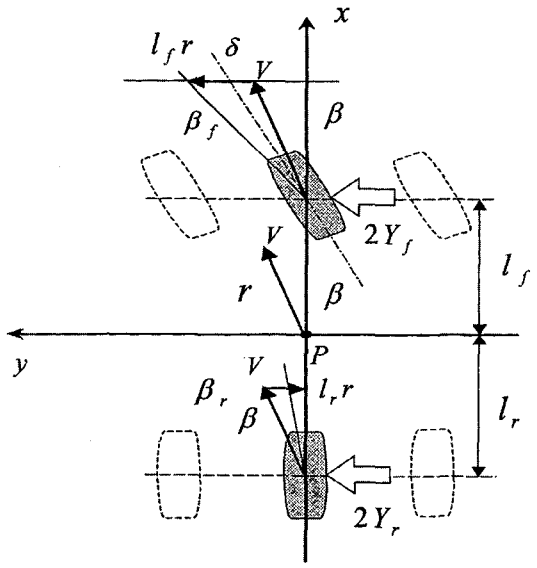

Fig. 8 Bicycle model for steering system modeling

substitute the reference signal in case of a straight lane. Before activating the steering control system, both the destination lane safety should be checked and verified for the unmanned vehicle (Yun and Kim, 1999).

The bicycle model in Fig. 8 is set up for the more precise and improved steering control. Rolling motion is neglected and the velocity of the vehicle is assumed to be constant and the vehicle drives on the uniform road. It is considered about the lateral motion and yawing motion only. If the vehicle, moving on the flat road, has acceleration about the lateral side, the acceleration occurs about the normal direction and the wheel has

acceleration, which is a cornering force (Ahn and Park, 2000).

If side slip angle assumed to be positive, the cornering forces of front and rear wheels are written by Eqs. (7), (8) on the basis of y axis as follows:

$$Y_f = -K_f\beta_f = -K_f\left(\frac{\beta + l_f\gamma}{V} - \delta\right) \tag{7}$$

$$Y_r = -K_r\beta_r = -K_r\left(\frac{\beta - l_r\gamma}{V}\right) \tag{8}$$

where, $Y_f = (Y_{f1} + Y_{f2})/2$, $Y_r = (Y_{r1} + Y_{r2})/2$, so it can be rewritten by

$$mV\frac{d\beta}{dt} + 2(K_f + K_r)\beta + \left\{mV + \frac{2}{V}(l_fK_f - l_rK_r)\right\}\gamma = 2K_f\delta \tag{9}$$

$$2(l_fK_f - l_rK_r)\beta + I\frac{d\gamma}{dt} + \frac{2(l_f^2K_f + l_r^2K_r)}{V}\gamma = 2l_fK_f\delta \tag{10}$$

with Eqs. (9) and (10), the equations of the vehicle yawing angle acceleration are to be induced. Thus, the equations through Laplace transformation are presented by

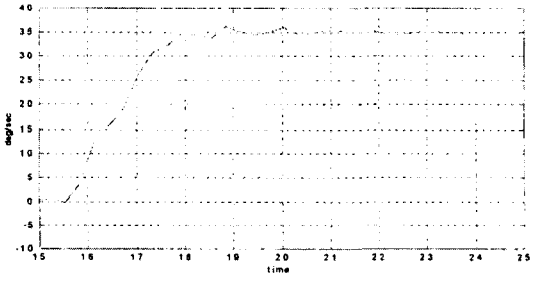

Fig. 9 Yaw rate profile by gyro sensor

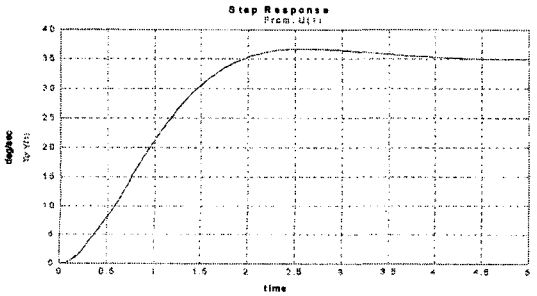

Fig. 10 Simulation result of transfer function

$$\frac{R(s)}{\Delta(s)} = \frac{2(mVl_fK_fs + (l_f^2K_f^2 + 2K_fK_r(2l_f - l_r)))}{mVI\left(s^2 + \frac{(2m(l_f^2K_f + l_r^2K_r) + 2I(K_f + K_r))s}{mIV} + \frac{4K_fK_rV^2}{mIV^2} + \frac{2(l_fK_f - l_rk_r)}{I}\right)} \tag{11}$$

where, the system parameter K_f, K_r and I are hard to find out as numerical values. Therefore, these parameters were chosen by an experimental method. If the vehicle has a step input, which causes lateral motion, output generated by the vehicle motion and it can be estimated from a gyro sensor. Figure 9 shows the result of step steer angle input acquired by a gyro sensor. Eq. (12) represents means the transfer function on a basis of the result (Yun and Kim, 1999; Kim, 2001).

$$G(s) = \frac{R(s)}{\Delta(s)} = \frac{97.3}{s^2 + 2.31s + 2.78} \tag{12}$$

With a result of real vehicle tests, the same value of step steer angle input is applied to simulation tests. Figure 10 shows the simulation result by MATLAB[R]. The result shows that steady state error and eigenvalue of the system is almost same, which means that the transfer function is reliable.

2.2 Sensor System

Figure 11 shows the signal definition of the system and the data flow [2] of Fig. 1, which represents the concept of another main theme in this research. It is focused on the sensor fusion and sensor system identification. Especially, longitudinal and lateral controls with a sensory system are fulfilled. The monitoring of the vehicle motion acquires information about 3 axis acceleration, position, velocity, heading angle and some environmental data, coming from several sensors. Acceleration sensor, ultrasonic sensor and gyro sensor output the analogous voltage, because these sensors detect physical term as like, acceleration, angle and sound, etc. These data should be converted to digital data by an A/D converter (Shim, 2001).

2.2.1 Laser sensor

Laser sensor is used to get the inter-vehicle distance of inter vehicles and detects an obstacle abruptly appearing in front of the unmanned vehicle.

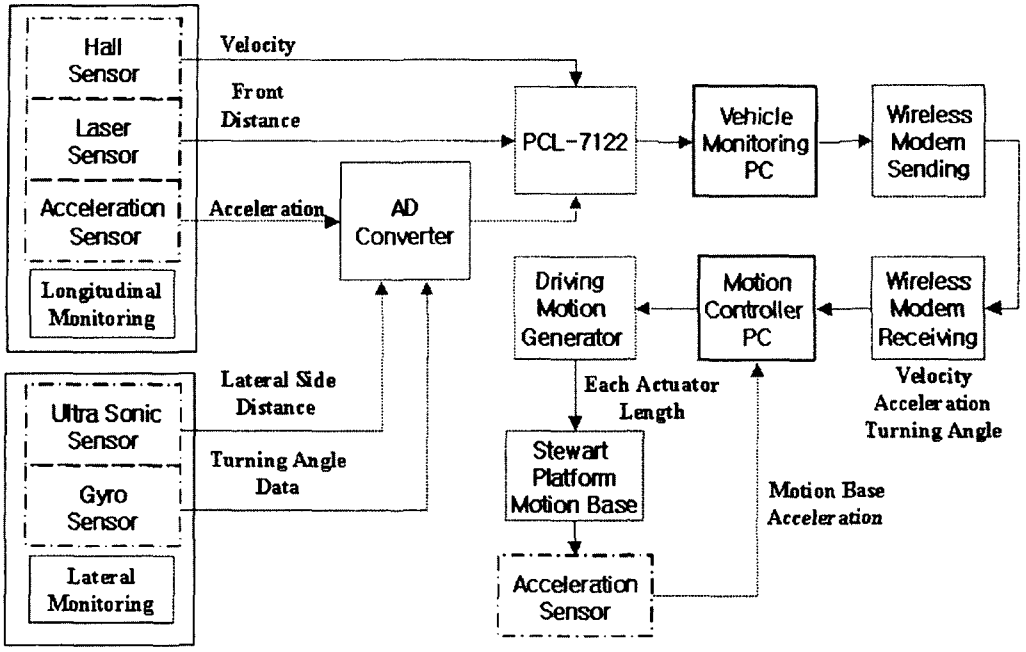

Fig. 11 Block diagram of sensor system

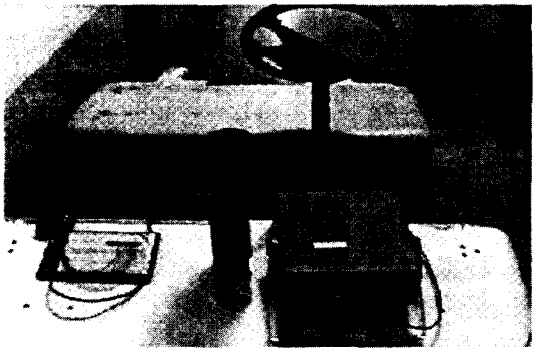

Fig. 12 Laser range finder

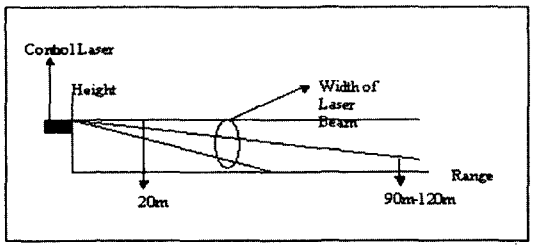

Fig. 13 Operation range of laser range finder

Figure 12 shows the laser sensor, which is attached on the front side of the unmanned vehicle and it used for the longitudinal control, because it produces data stream for keeping the system safety distance from the collision with front vehicle. However it has many error factors such as noise coming from electric magnetic interference of DC motor. Figure 13 shows the characteristic of the laser sensor, which is to shoot the beam to lower side from sensor position, so that the sensor should be set on the vehicle at the height of 1~1.5 [m] from ground (Yun and Kim, 2000 ; 2001 ; Shim, 2001).

2.2.2 Ultrasonic sensor

In this research, ultrasonic sensors are attached to the vehicle as shown in Fig. 14 for detecting side obstacles when the vehicle turns. Ultrasonic sensors detect the both side of wall around corridor, but inter wall space is so narrow that the vehicle cannot moves freely. Before using the ultrasonic sensor, it must be verified each sensor's characteristic, because each sensor generates different sensing output, although it has same specification, same model and same manufacturer. The distance signal of ultrasonic sensor is converted to digital data by an A/D converter and interfaced to the main computer. And the sensor's detecting distance and the angular detecting range look like cone.

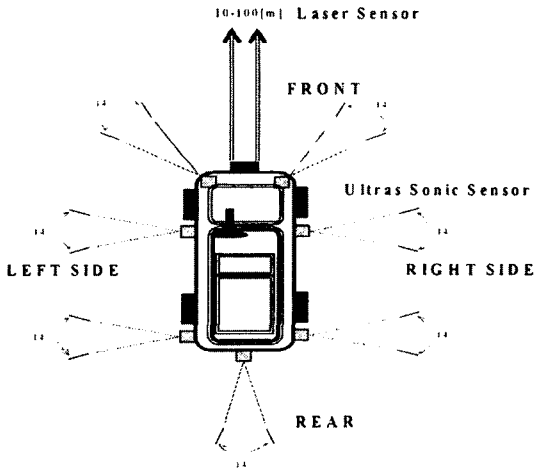

Fig. 14 Position of sonic & laser sensor

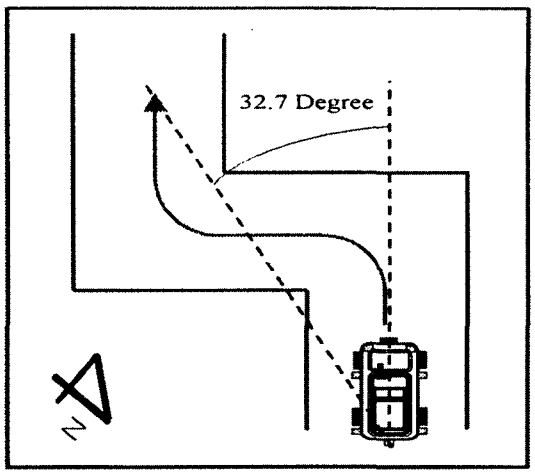

Fig. 15 Test road profile

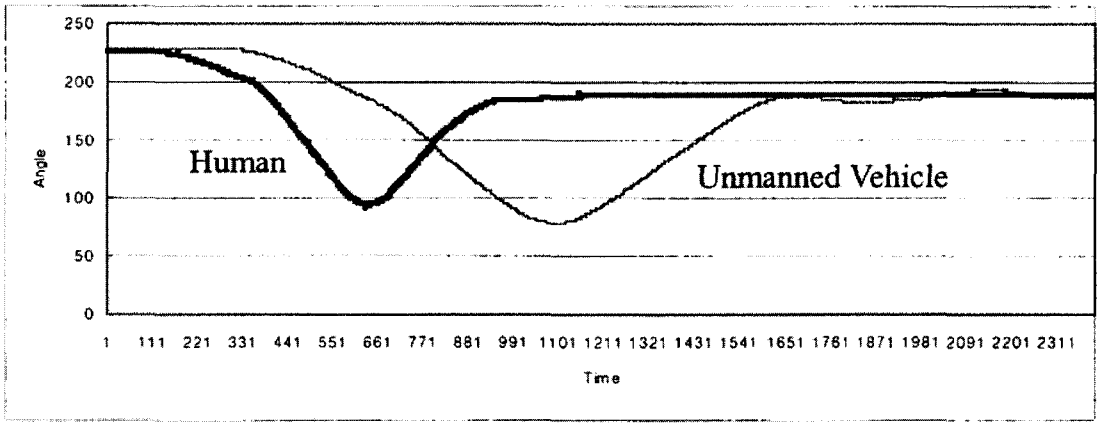

Fig. 16 Angular locus of unmanned & human driving

3. Test Evaluation

3.1 Lateral control test

Lateral control test is fulfilled in corridor of the building and Fig. 15 shows the test field's configuration. As a lateral control test, the unmanned vehicle driving test result is compared with the expert driver's test for finding the defect of the lateral control system.

Figure 16 shows the angular locus of the unmanned vehicle test and that of a human. The discrepancies of these results show the characteristic of a human driver and unmanned vehicle, which is managed by a sensory system, algorithm and actuator. The unmanned vehicle is dependent on the performance of actuator response and sensitivity of the sensory system. The unmanned vehicle data shows many angular position reimburse and the reaction is slower than that of human. Human detects the environment and road condition and he anticipates the control result (Yun and Kim, 2000; 2001).

For more precise lateral control, it requires a PID controller, etc. Eq. (13) shows the PID controller with the transfer function of Eq. (12), where K_p, K_i, K_d denote PID gain values, respectively.

$$G_C(s)=\frac{R(s)}{\Delta(s)}=\frac{97.3(K_d s^2+K_p s+K_i)}{s^3+(K_d+2.31)s^2+(K_p+2.78)s+K_i} \tag{13}$$

The settling time was reduced to 1 [sec] when we used the P, I, D gains with 2, 0, 1, respectively. Figure 17 shows simulation result based on those gain values.

3.2 Longitudinal control test

In real vehicle system, the velocity varies along the road friction, driving environment and battery charge ratio like shown in Fig. 18. It is very important that every test condition should be made with as same condition as possible. It shows the unmanned vehicle velocity profile when the desired velocity profile is applied to the traction system. Figure 19 shows the deceleration data at the speed of 12 [Km/h]. The first stage and increasing velocity zone shows minimal decelerating mode, but when the braking actuator applied, deceleration value rises abruptly, which data mean pitching motion of the vehicle.

To eliminate the unstable factor, a PID controller is applied to the traction system. The feedback system is set up through current velocity detecting from a hall sensor. If the voltage signal from the hall sensor assumes as $v_h(t)$, the state equation of the PID controller is given as

$$v_h(t) = k_h \omega \tag{14}$$

The Laplace transformed equations of the traction system are given by

$$V_h(s) = k_h \Omega(s) \tag{15}$$

$$U(s) = \left(k_p + \frac{k_i}{s} + k_d s \right) V_c(s) \tag{16}$$

If the parameters of Eq. (6) are applied to Eqs. (15), (16), the transfer function is obtained by

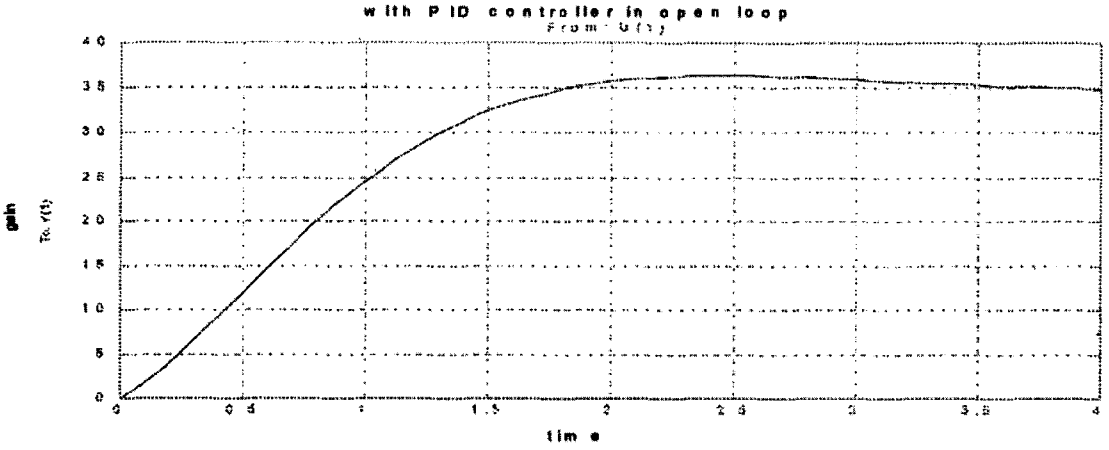

Fig. 17 Open loop system simulation with PID controller

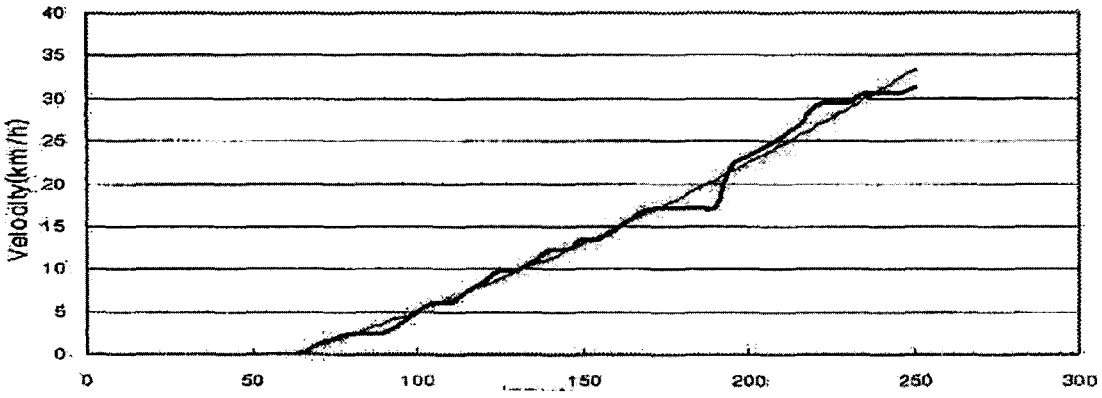

Fig. 18 Unmanned vehicle velocity profile

$$\frac{\Omega(s)}{R(s)}=\frac{5866.575(k_d s^2+k_p s+k_i)}{s^3+(4.55+k_d)s^2+(7.111+k_p)s+k_i} \quad (17)$$

In this research, the goal of the traction system controller is to obtain a settling time of within 2 seconds, a percent overshoot within 5%, and a steady state error within 1%. Through parameter tuning of the K_p, K_i, and K_d values by experiment, Figs. 20 and 21 show the simulation result on the basis of these acquired parameter conditions.

With gain values of k_p and k_d, which are verified with simulations, PD controller is applied to the real traction system on the vehicle. Figure 22 shows the result of the system response with the PD controller. It has a result of reducing

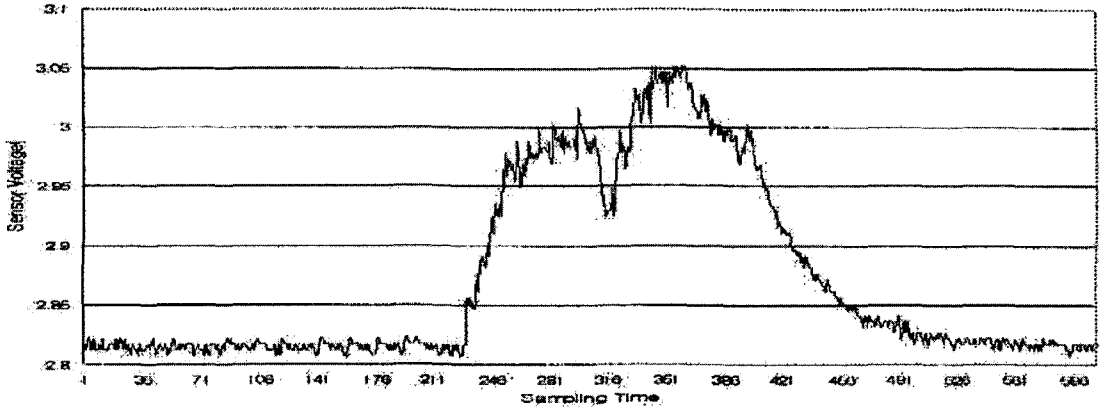

Fig. 19 Deceleration data of unmanned vehicle at 12[Km/h]

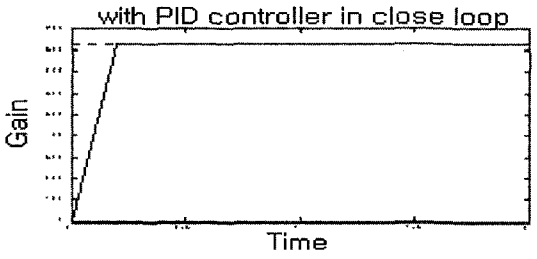

Fig. 20 Plant with PID controller

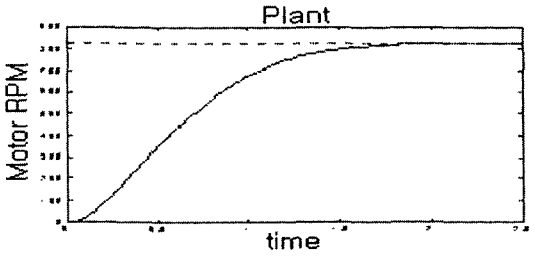

Fig. 21 Plant without PID controller

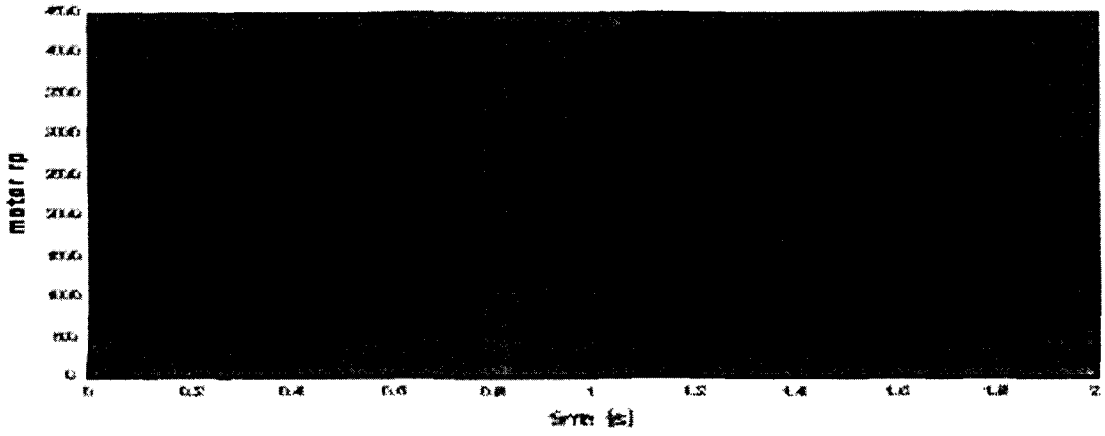

Fig. 22 Result of system response with controller

0.2 [sec] of settling time but not equal to the simulation results.

3.3 Sensor system test

Figure 23 shows the test result of the laser range finder. It started to measure an obstacle in 25 meters ahead of the wall. But a laser sensor generates a discrete-type signal, and thus it could cause an error in the measured signal. Because it is to display when the some ratio of distance change makes distinguished (Yun and Kim, 2000 ; 2001 ; Shim, 2001).

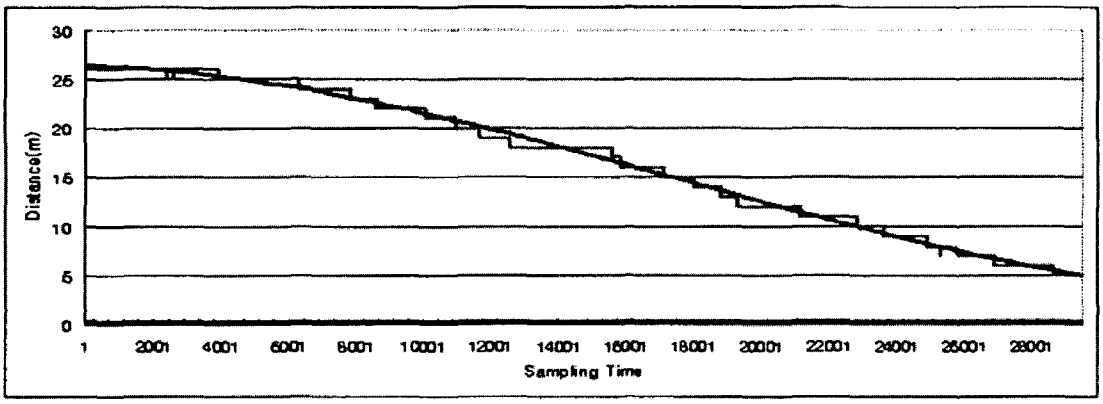

Fig. 23 Range change ratio in constant speed

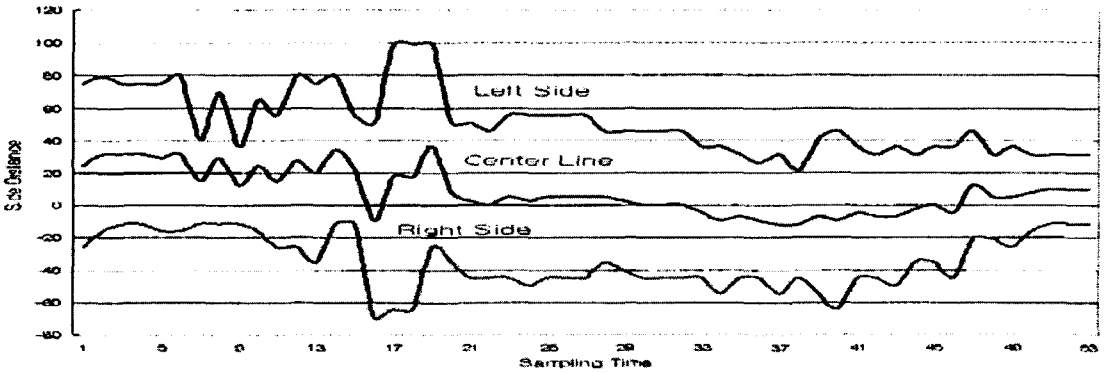

Fig. 24 Result of detecting the wall from ultrasonic sensor

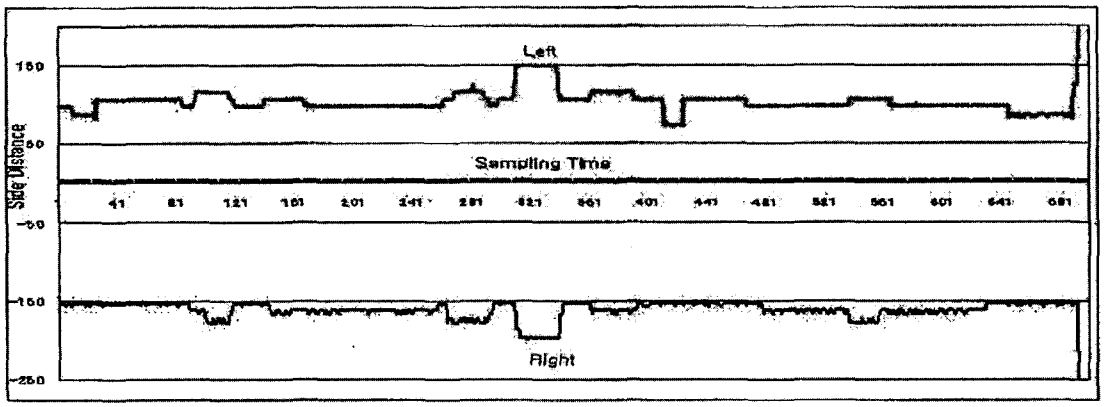

Fig. 25 Map generation with ultrasonic sensor

Figure 24 shows the algorithm test result of detecting the wall and finding the center position of the bilateral wall with an ultrasonic sensor without a gyro sensor. This result means that it is hard to make up the map data with only the ultrasonic sensor, because there are many steering control way of implementations. Figure 25 shows the map generation both with ultrasonic sensor and gyro sensor, which comes from vehicle driving locus and vehicle heading angle. It means that it requires two information at least for making a map data.

4. Conclusion

The work presented in this paper mainly deals with the unmanned vehicle design and associated design factors. The author designed the entire system and controller for longitudinal & lateral controls and evaluated the sensors. The analyzed results of the experiments for each part are as follows:

Longitudinal Control : Traction system modeling with the DC motor was accomplished, and the PID controller was applied to the vehicle with experimental parameter tuning. The performance improvement goal was to diminish the settling time to 0.2 [sec].

Lateral Control : The steering system was modeled and tuned controller parameters were determined experimentally. The performance improvement of the system was evaluated with simulation results. The results, obtained from the parameter tuning method, show that the settling time is diminished to 1 [sec]. However, for more precise control, it requires variable velocity control of the stepper motor, which is used for steering purpose.

Acknowledgment

This work was supported by the Brain Korea 21 Project.

References

Ahn Woo Sung and Park Hong Hyeon, 2000, "H_∞ Robust Yaw-Moment Control Based on Brake Switching for the Enhancement of Vehicle Performance and Stability," *Trans. of the KSME*, Vol. 24A, No. 8, pp. 1899~1909.

Kim Min Suk, 2001, "The System Modeling for Unmanned Vehicle & Autonomous Driving Technique by Ultrasonic Sensors," Master Thesis, Kookmin University.

Shim Jae Heung, 2001, "The System Design and Analysis of Unmanned Vehicle for the Tele-operating Control," Master Thesis, Kookmin University.

Yun Duk Sun and Kim Jung Ha; 2000, "The System Integration of Unmanned Vehicle & Driving Simulator for the Tele-Operated Vehicle System," *Proceeding of the Intl. Conf. of IASTED on RA2000*, pp. 197~201.

Yun Duk Sun and Kim Jung Ha, 2001, "The Performance Evaluation of Sensor & Actuator System for the Integration of Unmanned Vehicle and Driving Simulator," *Intl. Conf. of IASTED on Modeling & Simulation*, pp. 297~302.

Yun Duk Sun and Kim Jung Ha, 1999, "The Sensor Fusioning of Gyro Controller System for the Smart Vehicle," Intl. Conf. of IEEE on MFI, pp. 189~194.